Acta Chemica Scandinavica B 29 (1975) 797—810

Chemical Relaxation Studies on the System Liver Alcohol Dehydrogenase, NADH and Imidazole*

GEORGE H. CZERLINSKI,** MICHAL WAGNER, JAMES O. ERICKSON,*** and HUGO THEORELL

Department of Biochemistry, Northwestern University, Chicago, Illinois 60611, U.S.A. and Medical Nobel Institute, S-104 01 Stockholm 60, Sweden

Several years ago, Theorell and Czerlinski conducted experiments on the system of horse liver alcohol dehydrogenase, reduced nicotinamide adenine dinucleotide and imidazole, using the first version of the temperature jump apparatus with detection of changes in fluorescence. These early experiments were repeated with improved instrumentation and confirmed the early experiments in general terms. However, the improved detection system allowed to measure a slight concentration dependence of the relaxation time of around 3 ms. Furthermore, the chemical relaxation time was smaller than the one determined earlier (by factor 2). The data were evaluated much more rigorously than before, allowing an appropriate interpretation of the results.

The observed relaxation time is largely due to rate constants in an interconversion of ternary complexes, which are faster than three (of the four) dissociation rate constants, determined previously by Theorell and McKinley-McKee.[1,2] This fact contributed to earlier difficulties of finding any concentration dependence. However, the binding of imidazole to the binary enzyme-coenzyme complex can be made to couple kinetically into the interconversion rate of the two ternary complexes.

The observed signal derives largely from the ternary complex(es). A substantial fluorescence signal change is associated with the observed relaxation process, suggesting a relocation of the imidazole in reference to the nicotinamide moiety of the bound coenzyme. Nine models are considered with two types of coupling of pre-equilibria (none-all). Quantitative evaluations favor the model with two ternary complexes connected by an interconversion outside the four-step (bimolecular) cycle. The ternary complex outside the cycle has much higher fluorescence yield than the one inside. The interconversion equilibrium is near unity for imidazole. If it would be shifted very much to the side of the "dead-end" complex (as in isobutyramide?!), stimulating action could not take place.

Previously, we investigated thoroughly the chemical relaxation spectrum of the system of horse liver alcohol dehydrogenase (L-ADH) with nicotinamide adenine dinucleotide (NAD^+) and ethanol, observing primarily the slowest relaxation time over a wide range of reactant concentrations and pH.[3] Only indirect evidence was obtainable on the rate of interconversion among ternary complexes. We, therefore, decided to study the previously investigated chemical relaxation of the ternary complex between L-ADH, reduced nicotinamide adenine dinucleotide (NADH) and imidazole, projecting a possible correlation of this interconversion to the one expected in the previously mentioned system. No such correlation could be made, as the concentration dependence of the observed relaxation time was not particularly large. However, the equilibrium characteristics of the ternary complexes allowed some interesting mechanistic conclusions. Specifically, imidazole was selected as it forms a ternary complex of comparatively high fluorescence yield.

* The investigations were supported by a grant from USPHS/National Institutes of Health (1 RO1 MH20005—01).

** Requests for reprints should be addressed to the first author at 303 E. Chicago Avenue, Chicago, Illinois 60611, U.S.A.

*** Current Address: Optical Applications Laboratory, Varian Associates, Palo Alto, California 94303.

Furthermore, imidazole is known to stimulate the action of liver alcohol dehydrogenase. Finally, equilibrium and steady state kinetic data had already been determined by Theorell and McKinley-McKee [1,2] and were utilized in this investigation.

METHODS

Horse liver alcohol dehydrogenase was obtained from Boehringer (prepared according to the method of Dalziel [4]). The commercial preparation was centrifuged and dialyzed as described by Taniguchi *et al.*[5] The concentration of active sites in the stock solutions was determined as described by Theorell and Yonetani,[6] utilizing the ternary complex with pyrazole and NAD^+. In all cases was the binding capacity of the enzyme 100 % relative to its concentration determined spectrophotometrically. Anhydrous imidazole, Grade III, was obtained from Sigma Chemical Company and used without further purification. Phosphate buffers were prepared from the sodium salts as obtained from Baker Chemical Co., "Baker Analyzed" grade. Experiments were run at a constant ionic strength of 0.1 M and at 23.5 °C to coincide with the conditions established by Theorell and co-workers.[1,2,5-7] The pH was determined with a Radiometer pH meter, Model 26. The temperature jump apparatus used was based on the general coaxial design of Czerlinski,[8] following changes in fluorescence. As previously reported,[9] the excitation filter was a Kodak Glass filter type 18A, the emission filter a Kodak Wratten filter type 2B.

Considerable improvement of the signal-to-noise ratio has been obtained compared to the original instrument. The principal improvement was accomplished through an electronic refinement described recently.[10] Also, the General Electric BH6 Mercury arc lamp was replaced by the PEK107 Mercury arc lamp, selected for high performance (in conjunction with a Model 6274A hp/Harrison Power Supply). The employed power supply was operated either in the "constant current" mode, or in the "constant power" mode to further stabilize the energy output. It should be mentioned that the detection system still showed fluctuations of around 0.25 % of the total signal in a time range of 1 s, thus limiting the precision of repeat traces.

The oscilloscope traces were evaluated with Berman's computer program [11] for simulation, analysis and modeling, SAAM 23. Actual coordinate values for a given trace were obtained directly in digital form through the use of a Biomation 802 transient recorder, connected *via* a Dijiscan interface to a teletypewriter (ASR33) paper tape punch. The paper tape information was transferred onto disk for further evalution by computer programs. Up to 1024 points were compressed to a data matrix, not containing more than 50 abscissa-values: a typical section is shown in Fig. 1. A subordinate program extended these data (adding initial parameter estimates), to have them conform to the input format for SAAM 23 (executed in batch). Some more recent experiments were evaluated interactively from a teletypewriter, using a special fitting program.[12]

.2000	12.02133
.5000	26.91733
.8000	43.64267
1.1000	48.60800
1.4500	51.94000
1.8500	66.05200
2.2500	63.70000
2.6500	72.32400
3.1000	80.12480
3.6000	86.71040
4.1000	87.49440
4.6000	95.49120
5.1500	93.94933
5.7500	103.22667
6.3500	102.18133
6.9500	108.58400
7.6000	105.50400
8.3000	108.64000
9.0000	113.12000
9.7000	109.76000
10.4500	110.44600
11.2500	111.13200
12.0500	107.60400
12.8500	110.44600

Fig. 1. Listing of one data set for input into the SAAM 23 program. The first column gives values for the independent observable (time in ms). The second column denotes the dependent observable (signal change in mV). The data shown refer to chemical relaxation measurements on a mixture, consisting of 18 μN enzyme, 10 μN NADH, 5 mM imidazole, phosphate buffer of ionic strength 0.1, pH 8.0.

Program SAAM 23 returned the following value for the reciprocal of the chemical relaxation time: 0.383 ± 0.222 ms^{-1}.

The initial evaluation is based on the presumption of an exponential decay curve, $\Delta I(t) - \Delta I_1 \exp(-t/\tau_1) + \Delta I_0$ with $\Delta I(t)$ representing the signal change observed as a function of time (t). The ΔI_j, represent equilibrium signal changes, and τ_1 the chemical relaxation time constant. Time constant τ_1 is a function of the concentrations of L-ADH, NADH and imidazole. The quantitative relation depends upon the mechanistic details assumed by the investigator(s). After it became apparent (see discussion) that a monomolecular interconversion is associated with the ternary complex, two alternate schemes were analyzed further. Three models were considered for every scheme. Independent of earlier results from steady state kinetic experiments, two conditions were considered: no coupling-in of pre-equilibria (all other steps are much slower than the ones under consideration), full coupling-in of pre-equilibria (all independent other steps are much faster than the ones under consideration).

RESULTS

The experimental details were designed on the basis of earlier equilibrium studies of Theorell and McKinley-McKee.[1] Values for various equilibrium and rate constants were taken from the literature and are summarized in Table 1. The table shows the notations and subscripting for the equilibrium and rate constants, used in this paper. The direction of the flux for the dissociation rate constants is indicated directly in the column headings for the rate constants and refers also to the reaction step, described by the equilibrium constant in that column. The subscripting is unconventional in rapid chemical kinetics but introduced here for facilitating the needed transition to a generalized treatment of kinetic data. Positive and negative subscripts are frequently used in steady state kinetic treatments. However, the dissociation rate constants do not necessarily have negative subscripts. The equilibrium constants employed in the design of these experiments are graphically presented in Fig. 2. Specific relationships were derived (see Appendix I) to express the experimental apparent dissociation constants in

Table 1. Dissociation and rate constants[a] in the system of horse liver alcohol dehydrogenase (E), reduced nicotinamide adenine dinucleotide (R) and imidazole (I).

pH	Equil const. μM K_1	K_2	K_3	K_4
6	4200	2.01	470	0.23
7	3500	2.03	550	0.31
8	3600	2.20	680	0.41
9	3000	2.91	670	0.65
10	—	—	—	5[b]
	Rate const. s^{-1} k_{-1}	k_{+2}	k_{+3}	k_{-4}
	ERI→ ER+I	EIR→ EI+R	EI→ E+I	ER→ E+R
7	24.5	20.3	≥257	3.1
9	9	22	≥319	4.9

[a] Refs. 1,2; see especially pages 1846–1854; k_{+3} (pH 9) was computed under assumption that k_{-3} is not dependent upon pH, then $k_{+3}(\text{pH } 9) = k_{+3}(\text{pH } 7)\ K_{E,I}(\text{pH } 9)/K_{E,I}(\text{pH } 7)$.
[b] Ref. 18: In PO_4 $\mu = 0.1 + 0.1$ M glycine.

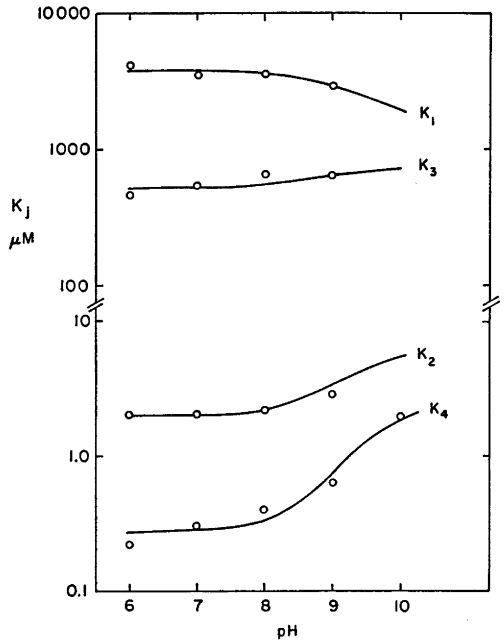

Fig. 2. Apparent dissociation constants K_1, K_2, K_3, and K_4 of binary and ternary complexes in the reaction of liver alcohol dehydrogenase with NADH and imidazole. The experimental points are those of Theorell and McKinley-McKee.[2] The theoretical curves are based on Scheme I of Appendix I with the following parameter values: $p\underline{K}_{-1} = 8.60$, $p\underline{K}_{-2} = 9.55$, $p\underline{K}_{-3} = 8.75$, $p\underline{K}_{-4} = 9.20$, $\underline{K}_{EH,R} = 9.28\ \mu M$, $\underline{K}_{EH,I} = 525\ \mu M$, $\underline{K}_{EHI,R} = 2\ \mu M$. The pH- independent constants are defined by the reaction scheme of Fig 3.

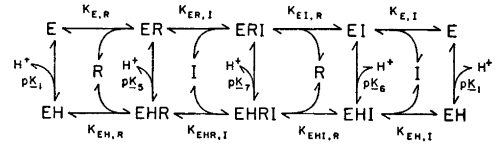

Fig. 3. Simplified reaction scheme to describe the pH-dependence of the dissociation constants in the reaction of horse liver alcohol dehydrogenase with NADH and imidazole. Values of specific constants are presented in the captions to Fig. 2. The reaction cycle involving free enzyme E and free reduced coenzyme R was introduced previously.[2] The remaining cycles are equivalent to mechanistic "interpolations". Values for the various dissociation constants are chosen such that the data of Theorell and McKinley-McKee are optimally approximated by them over the whole experimental pH-range. See Appendix I for quantitative relations.

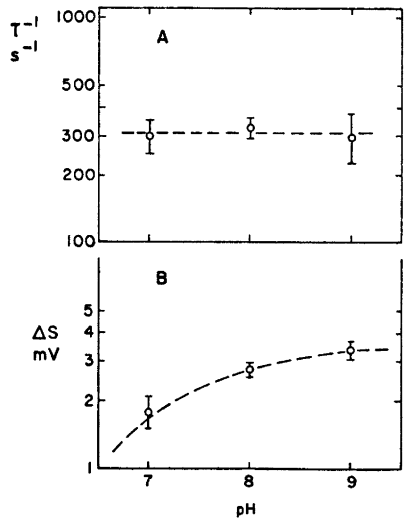

Fig. 4. The reciprocal of the chemical relaxation time as a function of pH in part A and the signal amplitude as a function of pH in part B of this figure. Conditions: 9.5 μN enzyme, 9.5 μM NADH and 1 mM imidazole; 25 °C final temperature, ionic strength 0.1 by phosphate (and a small amount of glycine). The curve indicates the "best fit" (no equation). Ordinate "bars" represent the total range of several repeat experiments. The ternary complex contributes most to the fluorescence.

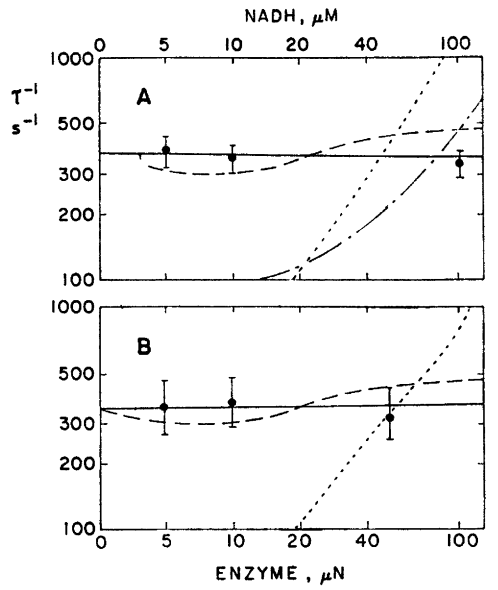

Fig. 5. The inverse chemical relaxation time as a function of the concentration of NADH (part A) and of enzyme (part B). The imidazole concentration was 5 mM and the concentration of the nonvarying component 10 μN; pH 7.0, ionic strength 0.1, 25 °C final temperature. The various theoretical curves are defined as follows: dotted for model *b*, full for model *e* (pos. root), dashed for model *d* (pos. root), dashed-dotted for model *a*. The dash-dotted curve in Fig. 5B is located outside the limits of the figure (below 100 s^{-1}). See Table 2.

terms of pH-independent constants. The underlying reaction scheme is shown in Fig. 3. One obtains theoretical curves which are shown in Fig. 2.

The results from the evaluation of the relaxation processes, utilizing the program SAAM 23, are summarized in Fig. 4 for pH-dependence of the inverse relaxation time and of the fluorescence equilibrium signal change. The horizontal line in Fig. 4A and the curve in Fig. 4B correspond to "best interpolations" without a specific model implied. Fig. 5. summarizes the measurements of the reciprocal relaxation time for coenzyme- and enzyme-dependence at pH 7. The curves here and in subsequent figures correspond to specific mechanistic models, which will be elaborated on under DISCUSSION. The experimental data are repeated in Fig. 6 with the curves referring to additional mechanistic models. The dependence of the observed reciprocal relaxation time upon the concentration of imidazole is presented in three different figures, namely in Fig. 7 for pH 7, in Fig. 8 for pH 8 and in Fig. 9 for pH 9. The various models tested are distributed over parts A and B of these three figures, showing their extent of fit to the experimental observations. Fig. 10B shows the reciprocal relaxation time plotted *versus* the imidazole concentration at three levels of NADH-concentration. Curves are here only inserted for a small number of mechanistic models. Fig. 10 A repeats the data of Fig. 7 and 8 with the theoretical curves referring to a combined evaluation (see below). To ascertain the concentration dependence at extreme concentration conditions, a large number of repetitions were necessary because of the low signal-to-noise ratio. Even then, the final value for the reciprocal of the relaxation time constant is only

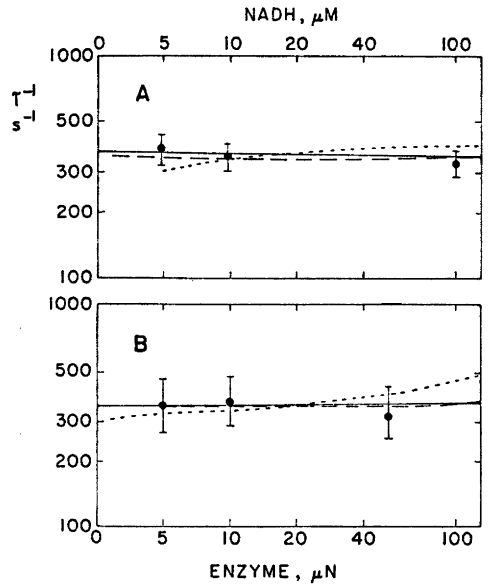

Fig. 6. Continuation of Fig. 5 with full line identical to full line in Fig. 5, the dashed line refers to Model *d*, the dotted one to Model *c*, for other details see Table 2.

accurate to ± 20 % at the concentration limits, to ± 10 % in between.

The most pronounced dependence of the reciprocal relaxation time upon the concentration of imidazole was found at pH 8. This pH seemed thus the optimal one for observing the concentration dependence. Subsequent experiments at increased coenzyme concentration (33, 166 and 330 μM NADH) did not allow to improve the extent of the dependence

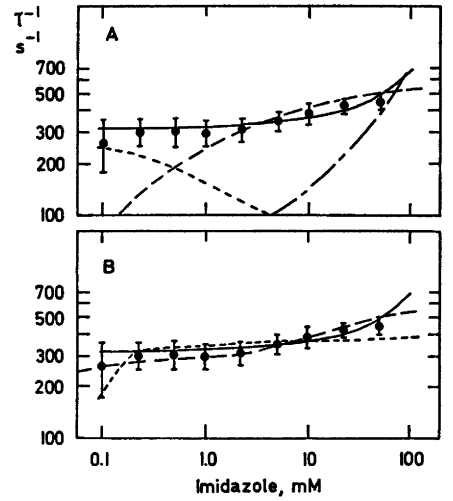

Fig. 8. The inverse chemical relaxation time as a function of the total concentration of imidazole at pH 8; 18 μN enzyme, 10 μN NADH, ionic strength 0.1, 25 °C final temperature. The theoretical curves are defined for Fig. 8A as in Fig. 5 and for Fig. 8B as in Fig. 6.

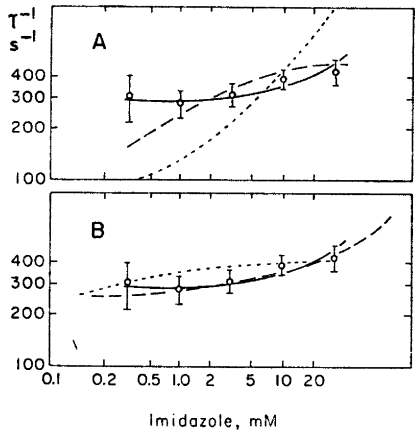

Fig. 7. The inverse chemical relaxation time as a function of the concentration of imidazole at pH 7.0 18 μM enzyme, 10 μN NADH, ionic strength 0.1, 25 °C final temperature. The various theoretical curves are defined for Fig. 7A as in Fig. 5 and for Fig. 7B as in Fig. 6.

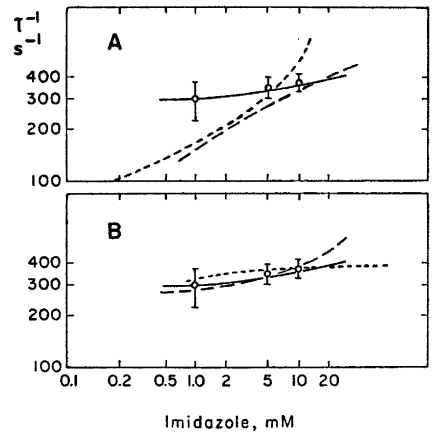

Fig. 9. The inverse chemical relaxation time as a function of the total concentration of imidazole at pH 9; 18 μN enzyme, 10 μN NADH, ionic strength 0.1, 25 °C final temperature. The theoretical curves are defined for Fig. 9A as in Fig. 5, and for Fig. 9B as in Fig. 6.

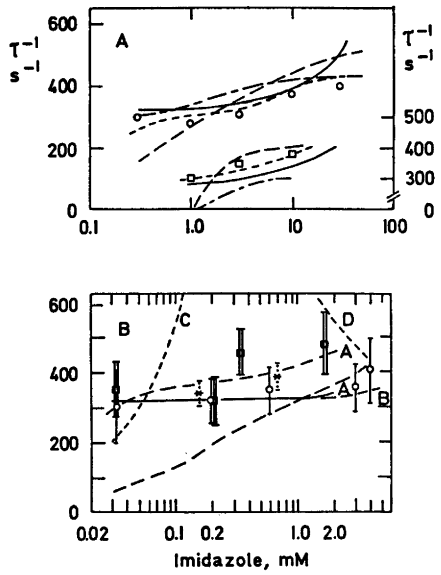

Fig. 10. The inverse chemical relaxation time as a function of the imidazole concentration. Fig. 10B refers to pH 8.0, 11.2 μN enzyme, phosphate buffer of ionic strength 0.1, 25 °C final temperature. Vertical "bars" refer to 33 μM NADH, vertical "double-bars" to 330 μM NADH and the two asterisks to 166 μM NADH. The various theoretical curves are defined as follows: full curve A with 33 μM NADH, dashed extension B of full curve A with 330 μM NADH, both for Model *d* (see Table 2). Dashed curve A refers to 330 μM NADH, dashed curve B to 33 μM NADH, both for Model *d*. Dotted curve C refers to 330 μM NADH and Model *b*, dotted curve D to 33 μM NADH and Model *a* (equivalent curve to 330 μM is off scale, meaning: above 600 s^{-1}). Other models have been tested, but fit even less. Fig. 10A. refers to fixed NADH at 10 μM, enzyme at 18 μN, phosphate buffer of ionic strength 0.1, 25 °C final temperature. The squares refer to pH 7.0 and the right scale, the circles to pH 8.55 and the left scale. The imidazole-dependence and the pH-dependence were fitted together, using the rate constants from the fit at pH 8.0 as initial estimates. The final values for the constants are insignificantly different from the initial estimates. The full theoretical curves refer to Model *f* (see Table 2) the dashed ones to Model *e*, the dotted ones to Model *d* and the dash-dotted ones to Model *a*. The curves for Model *b* are in shape similar to those of Model a, but deviate further from the experimental points than the dash-dotted curve does. The curves for Model *c* are outside the limits of the figure.

of the inverse relaxation time upon imidazole concentration, see Fig. 10A. However, these experiments clearly established the dependence of the relaxation time upon the concentration of NADH. This latter dependence transcends the assumption of only two steps competing in time range. A more rigorous analysis becomes then necessary, reserved for a specialized paper.[13]

Experiments were also conducted on mixtures of horse L-ADH with NAD^+ and ethanol in the presence of imidazole at pH 7.0. No influence of imidazole upon the reciprocal of the slowest relaxation time was observed, except at very high concentrations. Preliminary reports on the results were given at two meetings[14,15] Early experiments had not revealed a concentration dependence.[16]

DISCUSSION

1. Mechanistic principles. Already Theorell and McKinley-McKee [2] wrote the reaction of liver alcohol dehydrogenase, E, reduced nicotinamide adenine dinucleotide, R, and imidazole, I, as a four-step-cycle. The ternary complex ERI could be formed from E by two paths, one proceeding *via* ER, the other one *via* EI. Such a four-step cycle may be considered to be present in many enzyme reactions, equilibrating before attainment of the steady state. The heavy arrows in Fig. 11A notate an enzyme catalyzed isomerization reaction with competitive inhibition. The ternary complex ESI does not exist in ideal competitive inhibition, but may play a role in inhibitions of mixed character.

If one considers letter "I" to denote coenzyme, the system of Fig. 11B may be considered. An ideal ordered mechanism (heavy arrows) causes ES not to exist in the system. In any random (or even mixed) order mechanism, binary complex ES will have to be considered. A four-step-cycle of the described kind may thus be expected to appear quite commonly in enzyme kinetics.

One may now consider the time range of the equilibration of the four-step-cycle. The concentration dependence is expected to be considerable.[17] As only a small concentration dependence was found, presence of a monomolecular interconversion becomes highly prob-

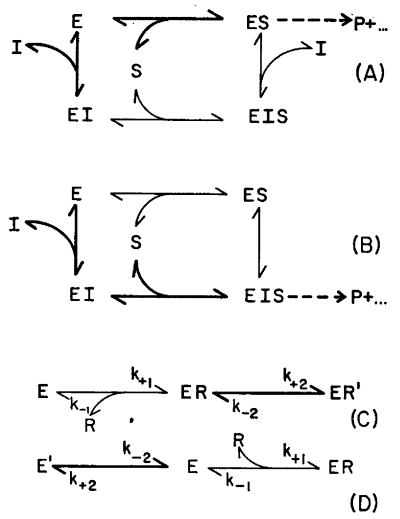

Fig. 11. Four reaction schemes are shown. The first two (A and B) relate to steady state kinetics, the last two (C and D) to chemical relaxation. Model A emphasizes competitive inhibition, but permits path *via* short-lived intermediate EI. Model B emphasized an ordered two-substrate reaction (S and I are substrates), but permits path *via* shortlived ES. Model C shows fast bimolecular step with slow isomerization of binary complex. Model D shows fast bimolecular step with slow isomerization of free enzyme. The dependence of the inverse relaxation time upon the concentration of reactant R is quite different for the two models C and D and will be used in the text to pinpoint the location of the observed isomerization.

able. Either one of the four enzyme containing components may in principle exist in two isomeric forms. However, specific patterns in the concentration dependence of the relaxation time may eliminate some choices. To illustrate the available patterns, two simple two-step-mechanisms are considered, namely those of Fig. 11 C and D. Case D shows two forms of free enzyme. The fast relaxation time, τ_1, is associated with the bimolecular step and the slow relaxation time, τ_2, with the interconversion step: $\tau_1 \ll \tau_2$.

If the time range of τ_2 is observed, the bimolecular reaction step is in pre-equilibrium and one obtains in case D (see eqn. (3−51) of Czerlinski [17]).

$$\frac{1}{\tau_2} = k_{-2} + k_{+2}\frac{[\mathrm{E}]+[\mathrm{R}]}{K_1+[\mathrm{E}]+[\mathrm{R}]} \qquad (1)$$

Similarly, one obtains in case C (see eqn. (3-57) of Czerlinski [16]):

$$\frac{1}{\tau_2} = k_{-2} + k_{+2}\frac{K_1+[\mathrm{E}]}{K_1+[\mathrm{E}]+[\mathrm{R}]} \qquad (2)$$

The rate constants are defined as shown in Fig. 11 C and D. If "Y" denotes a generalized component, equilibrium concentrations are indicated by [Y] and analytical concentrations by $C_\mathrm{y}°$. The equilibrium constant K_1 is defined by:

$$K_1 = \frac{k_{-1}}{k_{+1}} = \frac{[\mathrm{E}][\mathrm{R}]}{[\mathrm{ER}]} \qquad (3)$$

One may design the experiments such that:

$$C_\mathrm{R}° \gg C_\mathrm{E}° \qquad (4)$$

These analytical concentrations are defined by:

$$C_\mathrm{R}° = [\mathrm{R}]+[\mathrm{ER}]+[\mathrm{ER'}] \qquad (5)$$

$$C_\mathrm{E}° = [\mathrm{E}]+[\mathrm{E'}]+[\mathrm{ER}]+[\mathrm{ER'}] \qquad (6)$$

With $[\mathrm{E'}]\equiv 0$ for case C and $[\mathrm{ER'}]\equiv 0$ for case D. Condition (4) simplifies eqns. (1) and (2) to

$$(1/\tau_2)_\mathrm{C} = k_{-2} + k_{+2}C_\mathrm{R}°/(C_\mathrm{R}° + K_1) \qquad (7)$$

$$(1/\tau_2)_\mathrm{D} = k_{-2} + k_{+2}K_1/(K_1 + C_\mathrm{R}°) \qquad (8)$$

One realizes quickly that the concentration dependence of τ^{-1} upon $C_\mathrm{R}°$ is different for the two cases: Eqn. (7) shows an increase of τ_2^{-1} with increasing $C_\mathrm{R}°$ and with asymptotic approach of the limit $k_{-2}+k_{+2}$. Eqn. (8), applying to case D, shows in contrast to eqn. (7) a decrease of τ_2^{-1} with increasing $C_\mathrm{R}°$ with the value approaching asymptotically k_{-2}. This difference in the concentration dependence is crucial for differentiating among alternate mechanisms.

Returning to the pre-equilibration of the four-step-cycle in Fig. 11A, one may now consider four possibilities for isomerization, associated with either one of the four enzyme-containing components. One may further assume in zero approximation that bimolecular steps are rapid in comparison to monomolecular ones *and* that bimolecular steps adjoining monomolecular interconversions determine the concentration dependence (remote bimolecular steps do not contribute to the concentration dependence; any such contributions may in fact be treated as higher order corrections,

cf. eqn. (3-212) of Czerlinski [17]). The four possibilities show distinctly different dependencies of τ^{-1} *vs.* the analytical concentrations.

α. Isomerization of E. Case D applies with regard to inhibitor I *and* with respect to substrate S. The concentration dependence of eqn. (8) applies in both instances (R and I are equivalent).

β. Isomerization of ES. Case C (and thus eqn. (7)) applies with respect to component S and case D (and thus eqn. (8)) with regard to component R.

γ. Isomerization of ESI. Case C applies with regard to inhibitor I *and* with respect to substrate S. The concentration dependence of eqn. (7) applies thus in both instances.

δ. Isomerization of EI. This case shows a behaviour, which is inverted to case *β*: eqn. (7) applies with respect to component R and eqn. (8) with respect to component S.

The above discussion reveals that unique patterns of concentration dependence may be found. To what extent the underlying assumptions are fulfilled, will have to be investigated separately in every case. Our experimental results show the dependence of case *γ*: an isomerization among ternary complexes is thus most probable.

2. Mechanistic modeling

Although the small concentration dependence of the observed relaxation time speaks against assuming only a four-step-cycle, an exhaustive analysis of the four-step-cycle should be conducted nevertheless. Three specific models of the four-step-cycle will be considered, outlined in Fig. 12 *a*, *b*, *c*. Further details on these models will be discussed after the introduction of the nine basic models.

Even if a monomolecular interconversion is associated with the ternary complex, three different types of coupling of individual steps

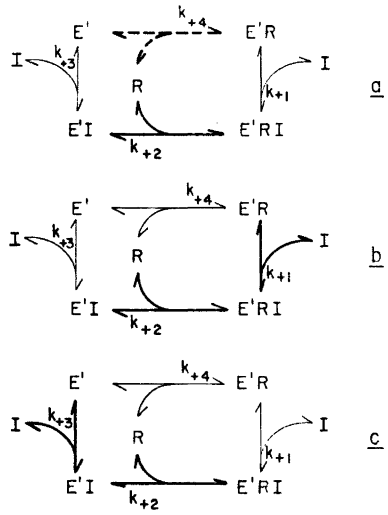

Fig. 12 Illustration of three four-step bimolecular cycles, used in the kinetic analysis. Heavy double-arrows indicate competing time ranges, which are considered to be possibly associated with the observed relaxation process. Model *a* describes the two steps with coenzyme-binding governing the time range of observation and the two steps involving Inhibitor I considered in pre-equilibrium. Only one relaxation process could be measured: the third relaxation time constant. Model *b* refers to the competition of the steps with k_{+1} and k_{+2}. Although k_{+4} is indicated as ordinary step it is ignored in the kinetic evaluation because of its established small contribution. Model *c* describes the steps with k_{+2} and k_{+3} kinetically competing.

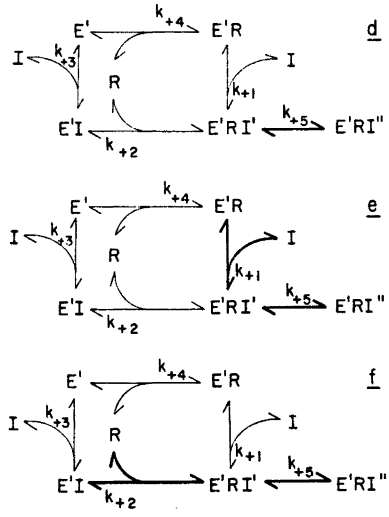

Fig. 13. Refers to models which involve the isomerization of a ternary complex to take place in a side-branch from a four-step bimolecular reaction cycle. Model *d* considers only one step governing the observed process, involving rate constants k_{+5} and k_{-5}. Model *e* considers the kinetic competition of two steps, namely those with the isomerization and with the binding of inhibitor involving rate constant k_{+1}. Model *f* refers to the kinetic competition of the isomerization with the adjoining bimolecular reaction step with rate constant k_{+2}.

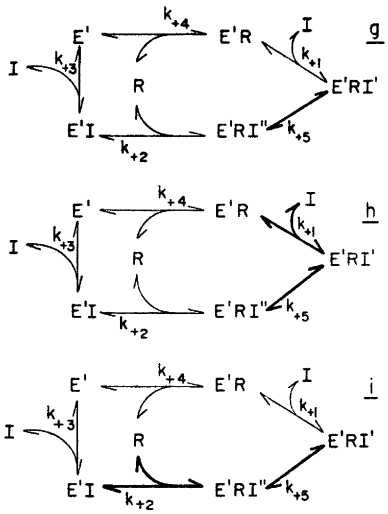

Fig. 14. Definition of reaction cycles of five steps with the interconversion among two ternary complexes being part of the five step cycle. Model *g* considers only the isomerization step being in the time range of the observation. Model *h* considers the adjoining binding step with inhibitor competing kinetically with the isomerization of ternary complexes. Model *i* considers the adjoining binding step with R (NADH) as kinetically competing with the isomerization of the two ternary complexes. The step with k_{+4} is considered as too slow to contribute significantly to the observed relaxation process.

have to be considered. The three types are shown in Fig. 13 as models *d*, *e* and *f*. The differentiation among these models derives also from the fact that only one relaxation process could be measured; no dependencies of other relaxation times are accessible.

The isomer of the ternary complex was shown outside a four-step-reaction cycle. However, two ternary complexes may also be considered as part of a five-step-reaction cycle. Differentiation of three types of coupling of individual steps leads to models *g*, *h* and *i* of Fig. 14.

Most of the nine models show two heavily drawn double-arrows. This notation refers to kinetically competing reaction steps. The system may be reduced to not less than two differential equations of the general type:

$$\frac{\mathrm{d}\Delta\xi_1}{\mathrm{d}t} = a_{11}\Delta\xi_1 + a_{12}\Delta\xi_2 \qquad (9)$$

$$\frac{\mathrm{d}\Delta\xi_2}{\mathrm{d}t} = a_{21}\Delta\xi_1 + a_{22}\Delta\xi_2 \qquad (10)$$

In these equations, the Greek symbol ξ_j refers to the "extent of the j-th reaction" and is associated with only one reaction step (concentrations may be involved in more than one reaction step: all components in model *a* participate in two reaction steps). Specific expressions for the a_{ij} will be given later on, where appropriate. One of the authors used $\mathrm{d}\xi$ recently in another kinetic study.[18] A general theory with programming implenentation on a digital computer is in preparation.[13]

The coefficients in (9) and (10) are utilized to compute the two reciprocal relaxation time constants (see eqns. (3-26) to (3-28) of Ref. 17):

$$1/\tau_{1,2} = \tfrac{1}{2}(a_{11}+a_{22})\ [1 \pm (1-b)^{1/2}] \qquad (11)$$

$$\text{with } b = \frac{4(a_{11}a_{22}-a_{12}a_{21})}{(a_{11}+a_{22})^2} \qquad (12)$$

The positive sign in front of the square root in eqn. (11) applies for subscript 1, the negative sign for subscript 2.

If only one heavy arrow is shown in a scheme, that step is considered alone with all remaining steps coupling in as pre-equilibria. If two heavy arrows are shown, two conditions for the remaining steps are considered. The remaining steps are either too slow to be included, or they are treated as coupled pre-equilibria. If the effects of coupled pre-equilibria are small, they may be undetectable below the error of the date and then appear as "too slow".

Expression for the a_{ij} are generally different for the various models. They will therefore now be discussed individually. Several special relations will be dicussed, as the various models are treated.

Model *a* considers the four-step cycle with those steps in pre-equilibrium, which involve the binding of imidazole, I. The cyclic sequence of the reaction steps makes one of the four steps dependent upon the others. A four-step cycle of the type of Model *a* can thus only have three relaxation time constants. Expressions for reciprocal relaxation times usually consist of only two terms. However, the slowest reciprocal relaxation time in a four-step cycle with one step dependent upon the

other three shows the reciprocal slowest relaxation time with four individual terms. The general expression was already discussed several years ago (see eqn (3-261) of Czerlinski [17]).

The following four equilibrium constants are defined with R = NADH and I = imidazole.

$$K_1 \equiv \frac{k_{-1}}{k_{+1}} = \frac{[E'R][I]}{[E'RI]} \quad (13)$$

$$K_2 \equiv \frac{k_{-2}}{k_{+2}} = \frac{[E'RI]}{[E'I][I]} \quad (14)$$

$$K_3 \equiv \frac{k_{-3}}{k_{+3}} = \frac{[E'I]}{[E'][I]} \quad (15)$$

$$K_4 \equiv \frac{k_{-4}}{k_{+4}} = \frac{[E'][R]}{[E'R]} \quad (16)$$

The Principle of Total Reversibility [19] applies to any reaction cycle, giving here:

$$\prod_{j=1}^{4} K_j = 1 \quad (17)$$

Eqn. (17) causes one of the prior equations to become dependent. Three equations for the analytical (total) concentrations are needed for the computation of equilibrium concentrations for all species:

$$C_E^\circ = [E'] + [E'R] + [E'RI] + [E'I] \quad (18)$$

$$C_E^\circ = [R'] + [E'R] + [E'RI] \quad (19)$$

$$C_I^\circ = [I] + [E'I] + [E'RI] \quad (20)$$

There are now six independent equations for the six unknown equilibrium concentrations. A subroutine for the computation of the six equilibrium concentrations with these six equations was described recently.[20]

The expression for the slowest relaxation time of this system was previously presented (eqn. (3-261) of Czerlinski [17]) and is repeated here with proper substitution:

$$1/\tau = k_{-4}\beta + k_{+2}\beta' + k_{+4}([E'] + [R]\alpha) + k_{-2}([E'I] + [R]\alpha') \quad (21)$$

The coefficients α, α', β, and β' were defined previously (eqns. (3-244), (3-245), (3-252), and (3-253) of Czerlinski [17]), but subsequently rearranged and are presented here, utilizing the symbols of model *a*. The following important relation exists among pairs of coefficients:

$$\alpha' = 1 - \alpha \quad (22)$$

$$\beta' = 1 - \beta \quad (23)$$

Furthermore:

$$\alpha = \left[1 + \frac{[I]([E'R] + [E'] + [I] + K_1)}{K_1([E'] + K_3^{-1}) + K_3^{-1}([E'R] + [I])}\right]^{-1} \quad (24)$$

$$\beta = \left[1 + \frac{[I]([E'R] + [E'] + [I] + K_3^{-1})}{K_1([E'] + [I]) + K_3^{-1}([E'R] + K_1)}\right]^{-1} \quad (25)$$

Eqn. (21) represents the exact solution for a "wide" separation of τ from any faster process.

The above equations contain equilibrium concentrations which are computed from pH dependent equilibrium constants and analytical concentrations numerically in a computer program, as described previously.[20] The pH-dependent dissociation constants are computed from pH-independent constants, as outlined in Appendix I. A numerical analysis revealed that the step with rate constant k_{+4} and k_{-4} contributes only a small part to the relaxation process. Under extreme conditions, the contribution barely approaches 10 %. As this amount is within the experimental error, one may consider the step with rate constant k_{+4} as too slow to be significant for the observed relaxation process. This means that the four-step cycle could be treated as a three-step sequence, involving forward rate constants k_{+1}, k_{+2} and k_{+3}.

Model *b* considers the mechanistic competition of the steps with the forward rate constant k_{+1} and k_{+2}. Eqn. (11) has to be applied together with the definitions

$$a_{11} = k_{+2} + k_{-2}([E'I] + [R]\alpha) \quad (26)$$

$$a_{22} = k_{-1} + k_{+1}([E'R] + [I]) \quad (27)$$

$$\alpha = ([E'] + [I])/([E'] + [I] + k_3^{-1}) \quad (28)$$

The terms a_{12} and a_{21} are omitted as they contain one of the two terms of the expressions for a_{ii}. Quite generally that term of the two-term expression has to be taken, the rate constant of which describes the flux *away* from the adjoining mechanistically competing step.

Model *c* represents a mechanistic competition between the reaction steps with rate constant k_{+2} and k_{+3}. Eqn. (11) thus has to be used again together with the coefficients:

$$a_{11}=k_{+2}\,\beta+k_{-2}([E'I]+[R] \quad (29)$$

$$a_{22}=k_{+3}+k_{-3}([I]+[E']) \quad (30)$$

$$\beta=([E'R]+[I])/([E'R]+[I]+K_1) \quad (31)$$

The expressions for a_{12} and a_{21} determined as described in the prior paragraph for model *b*.

Model *d* has no mechanistically competing steps, all reaction steps are considered in pre-equilibrium. The system of equations may thus be reduced to only one differential equation and the relaxation time constant becomes:

$$\tau^{-1}=k_{-5}+\gamma\beta k_{+5} \quad (32)$$

$$\gamma=([E'I]+[R])/([E'I]+[R]+K_2^{-1}) \quad (33)$$

although the expressions may be written in several ways, the shown one would reveal any concentration dependence most appropriately.

Model *e* shows two mechanistically competing steps, namely those with forward rate constants k_{+1} and k_{+5}. Eqn. (11) thus has to be applied together with

$$a_{11}=k_{-5}+k_{+5}\frac{[E'I]+[R]\gamma}{[E']+[R]\gamma+K_3^{-1}} \quad (34)$$

and the expression given in eqn. (27) plus a_{12} and a_{21} as described above.

Model *f* shows the alternate type of mechanistic competition with forward rate constants k_{+5} and k_{+2} involved. Eqn. (11) again has to be used together with

$$a_{11}=k_{-5}+\beta k_{+5} \quad (35)$$

$$a_{22}=k_{+2}+k_{-2}([E'I]+\alpha[R]) \quad (36)$$

Model *f* completes one class of three models.

The addition of the monomolecular interconversion requires a redefinition of K_1 and K_2 for the kinetic evaluations *only*. The redefinition derives from the new constant

$$K_5\equiv\frac{k_{-5}}{k_{+5}}=\frac{[E'RI]}{[E'RI'']} \quad (37)$$

One may add the definition:

$$[E'RI]=[E'RI']+[E'RI''] \quad (38)$$

A "prime" may be used to define the "kinetic" (or "reduced) equilibrium constants.

$$K_1'=\frac{[E'R][I]}{[E'RI']}=K_1(1+K_5^{-1}) \quad (39)$$

$$K_2'=\frac{[E'RI']}{[E'R][I]}=K_2/(1+K_5^{-1}) \quad (40)$$

Equilibrium constants K_1 and K_2 in eqns (31) and (33) will have to be replaced by K_1' and K_2' from eqns (37) and (38) for models *d*, *e* and *f*.

Model *g* shows only one reaction step to be considered in the time range of observation. The system of equations may therefore be reduced to one differential equation with the reciprocal relaxation time given by

$$\tau^{-1}=\gamma k_{+5}+\beta k_{-5} \quad (41)$$

Model *h* shows two mechanistically competing steps, involving k_{+1} and k_{+5}. Eqn. (11) applies with the expression

$$a_{11}=k_{-5}+k_{+5}\frac{[E'I]+[R]\alpha}{[E'I]+[R]\alpha+K_3^{-1}} \quad (42)$$

and eqn. (27) for a_{22} plus a_{12} and a_{21} as described above.

Model *i* shows two mechanistically competing steps, namely those with forward rate constants k_{+5} and k_{+2}. Thus, eqn. (11) applies with the definitions

$$a_{11}=K_{-5}+\beta+K_{+5} \quad (43)$$

while for eqn. (36) applies: a_{12} and a_{21} are used as described earlier.

Models *g*, *h* and *i* involve K_2' for K_2', as defined in eqn. (37). However, K_2' is differently defined and a new expression has to be used, namely:

$$K_1'=\frac{[E'RI'']}{[E'I][R]}=K_2/(1+K_5) \quad (44)$$

This new kinetic dissociation constant is to be used in the expressions for models *h* and *i*.

All the above equations apply to the limiting case of pre-equilibration of those steps, which are not mechanistically competing. The other limiting case refers to the condition that the not mechanistically competing steps are too slow for having any effect in the time range of observation. This condition is obtained computationally by

$$\alpha=\beta=\gamma=1.0 \quad (45)$$

There is one additional restriction in reference to the use of eqn. (45) for model *e*: eqn. (35)

Table 2. Survey of models employed.

Model	Relevant eqns.	No pre-equilibria assumed Fitted values (in s^{-1}) for a_{11}-term	a_{22}-term	a Fit *	With pre-equilibria assumed Fitted values (in s^{-1}) for a_{11}-term	a_{22}-term	b Fit *
a	(22)	–	–		$k_{+3}=14.1$ β $k_{-2}=K_2k_{+2}$	$k_{+4}=2.63$** $k_{-4}=K_4k_{+4}$	– – –
b	(11, 26, 27)	$k_{+1}=5.03$ α $k_{-1}=K_1k_1$	$k_{+2}=131.6$ $k_{-2}=K_2k_{-2}$ **	–	$k_1=5.5$ α $k_{-1}=k_1K_1$	$k_{+2}=97$ $k_{-2}=K_2k_2$ **	– –
c	(11, 29, 30)	$k_{+2}=263$ β $k_{-2}=K_2k_{+2}$	$k_{+3}=331$ β $k_{-3}=K_3k_{+3}$	– –	$k_{+2}=25$ $k_{-2}=K_2k_{+2}$	$k_{+3}=351$ β $k_{-3}=K_3k_{+3}$	– –
d	(32)	–	–		$k_{+5}=217$ β $k_{-5}=77$	(also in pre-equil.)	– –
e	(11, 27, 34)	$k_{+5}=177$ α $k_{-5}=125$	$k_{-1}=14.4$ $k_{+1}=k_{-1}/K_1'\phi$	+ + +	$k_{+5}=234$ β $k_{-5}=79$	$k_{-1}=14.6$ $k_{+1}=k_{-1}/K_1'\phi$	–
f	(11, 35, 36)	$k_{+5}=179$ α $k_{-5}=161$	$k_{+2}=0.15$ $k_{-2}=K_2'k_{+2}$ α	+ +	$k_{+5}=202$ β $k_{-5}=220$	$k_{+2}=0.19$ β $k_{-2}=K_2'k_{+2}$	–
g	(41)	–	–		$k_{+5}=243$ β $k_{-5}=670$	(also in pre-equil.)	–
h	(11, 27, 42)	$k_{+5}=177$ β $k_{-5}=125$	$k_{-1}=24.4$ $k_{+1}=k_{-1}/K_1'\phi$	+	$k_{+5}=138$ $k_{-5}=191\phi$	$k_{-1}=13.6$ $k_{+1}=k_{-1}/K'\phi$	+
i	(11,30,43)	$k_{+5}=183$ α $k_{-5}=163$	$k_{+2}=0.90$ $k_{-2}=K'_2k_{+2}$ α	+ +	$k_{+5}=207$ β $k_{-5}=206$	$k_{+2}=0.15$ β $k_{-2}=K_2'k_{+2}$	– –

* "Fit" takes into account all accessible parameters, including errors of parameter values, magnitude of "Sum-squares of residuals" and the visual agreement of theoret. curves with the data, covering a total of *18* data values for every entry in the table. The entries in this column refer to the fitted values listed to the left with the following definitions: + + + indicates the "best of all fits." + + indicates a reasonably good fit; any entry of "+ +" aside of "+ + +" does not allow the model with "+ + +" to be labeled "uniquely fitting." + indicates a fit which cannot be completely ruled out as referring to a possible model. A large number of additional data from suitably extended experiments could possibly provide further information on the ultimate validity of this model. – indicates a fit which would rule out the underlying model from further consideration. – – indicates a bad fit. – – – indicates the worst of all fits.

** The value refers to a bimolecular rate constant in the units M^{-1} s^{-1}.

β standard errors are about half the size of the given parameter-values.

α standard errors are of the size of the given values.

ϕ The computer program returned errors for this rate constant, which are substantially larger than those returned for the rate constants k_{+5} and k_{-5}. To express these errors properly, an undimensioned number ϕ has to be used, which is both a factor in a product and a divisor in a quotient *with* a parameter value χ. If $(\phi-1) \ll 1$, it is directly related to the standard error ε by: $\varepsilon=(\phi-1)\chi$, Where ϕ is actually listed, it is of the order of 5 to 10 (applies directly *only* to the equilibrium constant in the expression).

ought to be employed in place of eqn. (34). This replacement is obvious from the inspection of the factor of k_{+5} in eqn. (34), which describes a pre-equilibrium. As all models and underlying mathematics have now been described, the equations may be employed in data fitting programs.

3. Evaluation of goodness of fit. The experimental observable, like the reciprocal relaxation time, may be generally defined as λ_i*. The corresponding computed value, which is dependent upon the independent variables C_E°, C_R°, C_I° and pH, is similarly defined by λ_i°. One may then form the following relation for all points, considered in the fitting process:[21]

$$\sigma_m = \sum_i (\lambda_i^* - \lambda_i^\circ)^2 \qquad (46)$$

The fitting program reduces σ_m to a minimum for all points included in the fitting procedure. Subscript m refers to the model number. Comparisons are made between different sets of data, including also a consideration of standard errors of the parameters. The results of

the least squares fits are shown in Figs. 5 to 10. An overall evaluation is presented in Table 2, indicating how well individual models can be brought into agreement with the experimental results. Model *e* fits best, if no pre-equilibration is assumed. However, the data will not allow to define Model *e* as unique, as the fit for Models *f* and *i* can not be labelled poor enough in reference to Model *e*. It is quite possible that three reaction steps compete mechanistically in the time range of observation. However, there are then too many adjustable kinetic parameters, the precise determination of which is not justified by the available data. It is doubtful that the relaxation time can be measured over a sufficiently broad range of concentration, to permit consideration of three mechanistically competing steps. However, concentration ranges may be found where some concentration dependence upon both imidazole and coenzyme can be detected.

The measured relaxation process is associated with a substantial fluorescence signal change. This signal change is interpreted as largely due to a change in fluorescence yield, as the weakly fluorescing ERI′ converts to the highly fluorescing ERI″ (the "dead-end complex" in models *d*, *e* and *f*). Imidazole thus rearranges in the ternary complex in a way, which diminishes vibrational energy losses from the electronically excited nicotinamide moiety of bound NADH. The equilibrium constant of the interconversion among the two ternary complexes is close to 1.0. If the equilibrium would be shifted to the weakly fluorescing complex ERI′ (by an inhibitor related to imidazadole or by a change in the solution medium), stimulation of the overall kinetics would be further increased to eventually reach a limit of factor 2. On the other hand, if an inhibitor should favor formation of the highly fluorescing compound ERI″, the fast equilibration among the two ternary complexes would remove the dissociating ERI′ from the reaction path and the stimulatory effect upon the overall reaction would diminish and may even disappear completely. Certainly, one should search for effectors, which stimulate the ethanol metabolism further. More data on different inhibitors have to be collected, to more precisely define the structure of the optimal stimulator.

It should be mentioned that the "Fits" in column a of Table 2 are generally significantly better than the "Fits" in column b. This is to be expected as all values for k_{+5} and k_{-5} exceed 100 s^{-1}, while the remaining adjoining rate constants k_{-1} and k_{+2} are below 25 s^{-1} (compare also the corresponding steady state rate constants in Table 1).

The results of Table 2 will now be compared with the earlier ones summarized in Table 1. To make a comparison with data from steady state kinetic experiments feasable, one has to establish quantitative relations between the model for steady state kinetics and the model for chemical relaxation experiments. Such relations were considered previously.[22] Two situations were discussed there: One reactant in a bimolecular reaction is present in two forms, only one of which participates in the reaction; the product in a bimolecular reaction (the binary complex) is present in two forms, only one of which is directly involved in the bimolecular reaction step. The latter case applies here. If a rate constant with a "prime" denotes the one from steady state kinetics, one equates on the basis of model *e*: $k_{+1}' = k_{+1}$ and $k_{-2}' = k_{-2}$. The reverse rate constants are with the definitions of model *e*:

$$k_{-1}' = k_{-1}/(1 + K_5) \quad (47)$$

$$k_{+2}' = k_{+2}/(1 + K_5) \quad (48)$$

These equations imply $k_{+5} \gg k_{-1}, k_{+2}'$ which is fulfilled with sufficient approximation. As k_{+2} is not kinetically competing with k_{+5} in the observable time range for model *e*, eqn. (48) can not be applied. One obtains from Table 2 with eqn. (37): $K_5 = 0.706$ and thus with eqn. (47) $k_{-1}' = 8.47$ s^{-1}. This value is rather close to the corresponding value, listed in Table 1 for pH 9. The agreement between results from steady state kinetics and those from chemical relaxation kinetics is thus quite good.

APPENDIX I

The pH-dependence of the apparent equilibrium constants. Fig. 3 of this paper presents an elaborate reaction scheme, containing both protonated and unprotonated enzyme forms. This scheme may be directly derived from the results of Theorell and McKinley-McKee [1]

and implies the assumption of only one active-site-linked proton. The captions to Fig. 3 define the set of constants, which has to be used to obtain the proper pH-dependent constants. The latter are defined in terms of the constants in Figure 3 by the four equations:

$$K_4 = \frac{([EH]+[E])[R]}{[EHR]+[ER]} = K_{EH,R}\frac{1+\underline{K}_1[H^+]}{1+\underline{K}_5[H^+]} \quad (A\text{-}1)$$

$$K_1 = \frac{([EHR]+[ER])[I]}{[EHRI]+[ERI]} = K_{EHR,I}\frac{1+\underline{K}_5/[H^+]}{1+\underline{K}_7/[H^+]} \quad (A\text{-}2)$$

$$K_3^{-1} = \frac{([EH]+[E])[I]}{[EHI]+[EI]} = K_{EH,I}\frac{1+\underline{K}_1/[H^+]}{1+\underline{K}_6/[H^+]} \quad (A\text{-}3)$$

$$K_2^{-1} = \frac{([EHI]+[EI])[R]}{[EHRI]+[ERI]} = K_{EHI,R}\frac{1+\underline{K}_6/[H^+]}{1+\underline{K}_7/[H^+]} \quad (A\text{-}4)$$

The apparent dissociation constants are also defined in eqns. (13) to (16).

The "best" values for the various dissociation constants are given in the caption to Figure 2. The constants $\underline{K}_2^{-1}$ and $\underline{K}_{EHI,R}$ are *not* independent of the other constants. The apparent constants can be determined with the values in the mentioned table for any pH in the range $6.0 \leq$ pH ≤ 10.0 (values for the upper limit are extrapolated and therefore more speculative than values below this limit). The value for $p\underline{K}_6$ represents a "lower limit"; if $\underline{K}_6$ is decreased, both $\underline{K}_{E,I}$ and $\underline{K}_{EI,R}$ would change to satisfy the condition among dissociation constants in a symmetric reaction cycle. Fig. 2 shows the agreement between experimental points and theory for a given set of pH independent constants.

The pH-dependent equilibrium constants are computed in a separate subroutine, labelled "THEØR", whenever a change in the value of the pH is detected by the main program. The new constants are then used for the computation of equilibrium concentrations of all components and for the computation of the relaxation times, according to the various models.

REFERENCES

1. Theorell, H. and McKinley-McKee, J. S. *Acta Chem. Scand. 15* (1961) 1811.
2. Theorell, H. and McKinley-McKee, J. S. *Acta Chem. Scand. 15* (1961) 1834.
3. Czerlinski, G. H. and Erickson, J. O. *Enzyme Commun. In press.*
4. Dalziel, J. *Acta Chem. Scand. 12* (1958) 459.
5. Taniguchi, J., Theorell, H. and Åkesson, Å. *Acta Chem. Scand. 21* (1967) 1903.
6. Theorell, H. and Yonetani, T. *Biochem. Z. 338* (1963) 537.
7. Shore, J. D. and Theorell, H. *Arch. Biochem. Biophys. 116* (1966) 255.
8. Czerlinski, G. *Rev. Sci. Instrum. 33* (1962) 1184.
9. Czerlinski, G. In Schwert, G. W. and Winer, A. D., Eds., *The Mechanism of Action of Dehydrogenases*, Univ. Kentucky Press, 1970, p. 131.
10. Czerlinski, G. *Rev. Sci. Instrum. 39* (1968) 1730.
11. Berman, M. In Stacy, R. and Waxman, B., Eds., *Computers in Biomedical Research*, Academic, New York 1965, Vol. 2, Chapter VIII.
12. Shah, P., Haidle, R. and Cherlinski, G. *Proc. Nat. Computer Conf!* Chicago 1974, pp. 107–114.
13. Wagner, M. and Czerlinski, G. *In preparation.*
14. Czerlinski, G. and Erickson, J. O. *9th Int. Congr. Biochem.*, Stockholm 1973, 2 r 5, p. 109.
15. Erickson J. O. *Fed. Proc. Fed. Amer. Soc. Exp. Biol. 30* (1971) 1239 ABS.
16. Czerlinski, G. and Theorell, H. *ACS Meeting Chicago 1961*, Abstracts p. 11T.
17. Czerlinski, G. *Chemical Relaxation*, Dekker, New York 1966.
18. Zablinski, R., Tatti K. and Czerlinski, G. H. *J. Biol. Chem. 249* (1974) 6125.
19. Skrabal, A. *Homogenkinetik*, Steinkopff, Dresden 1941.
20. Czerlinski, G. H. and Kobbe, R. *Comput. Programs Biomed. 3* (1973) 87.
21. Wagner, M., Czerlinski, G. and Pring, M. *Comput. Biol. Med. 5* (1975) 105.
22. Czerlinski, G. H. and Malkewitz, J. *Biochemistry 4* (1965) 1127.

Received February 1, 1975.